of Hartree–Fock theory with a split-valence plus polarization basis set to determine the equilibrium geometry and zero-point vibrational energy of a given molecule or radical. With use of the geometry determined at the Hartree–Fock level, the total energy is determined with fourth-order Møller–Plesset perturbation theory (MP4). Bond additivity corrections (BAC) are added to the theoretically calculated energies. The resulting heats of formation have been demonstrated to be accurate to within 3 kcal/mol.[54] Relative energies in a homologous series would have greater accuracy.

These calculations have confirmed some of the important assumptions used in applying group additivity concepts, but they have also revealed differences that are not in agreement with the additivity principle.[53] For example, Melius has found that ROO–H bond energies are the same for different R groups, a result predicted by the no-next-nearest-neighbor assumption of group additivity. For R = H, CH_3, and OH, the ROO–H calculated bond strengths differ by about 1 kcal/mol.[53] However, $R-O_2$ bond strengths in alkyl peroxy radicals were found to *increase significantly* with increasing complexity of the R group. The $C_2H_5-O_2$ bond energy was determined to be 3.3 kcal/mol greater than that of the CH_3-O_2 bond, and the i-$C_3H_7-O_2$ bond was estimated to be an additional 1.7 kcal/mol stronger than the $C_2H_5-O_2$ bond based on analogous trends found for R–OH bonds for the same R groups. This trend is not predicted by group additivity concepts. The intrinsic $R-O_2$ bond strengths calculated by Melius ($\Delta H°(0)$) are about 4 kcal/mol lower than measured values: 26.3 kcal/mol for CH_3-O_2 vs. 30.7 from experiment,[29] and 31.3 kcal/mol (extrapolated) for i-$C_3H_7-O_2$ vs. 36.4 measured in the current study. Because of this disagreement, it is uncertain whether the heat of formation of i-$C_3H_7O_2$ predicted by group

additivities is actually an overestimate, but it is likely that group methods lead to significant inaccuracies when applied to RO_2 radicals.

This study has yielded the first direct determination of the enthalpy change associated with an alkyl radical–oxygen equilibrium, and hence it provides the most exacting test to date of group additivity methods for predicting the energy changes associated with reactions in this class. Future studies on additional equilibria involving other alkyl radicals and oxygen should help to establish more clearly the source or sources of the small but notable disagreement between experiment and estimation.

III. The Stability of i-$C_3H_7O_2$ and Combustion Modeling. The stability of RO_2 radicals in combustion systems is often characterized by a "ceiling temperature".[13] It is that temperature at which the equilibrium constant for reaction 1 predicts that the ratio of pressures $P(R)/P(RO_2) = 1$ for the oxygen pressure in the reacting system. It is a useful parameter for estimating the dividing temperature between low- and high-temperature combustion mechanisms. The results of this study indicate that the i-$C_3H_7O_2$ is more stable towards dissociation than was predicted previously. The ceiling temperature for the i-$C_3H_7 + O_2 \leftrightarrow$ i-$C_3H_7O_2$ equilibrium calculated by using the results of this study is 40 °C higher than earlier estimates.

Electrocatalysis of Proton-Coupled Electron-Transfer Reactions at Glassy Carbon Electrodes

George E. Cabaniss,[†] **Alex A. Diamantis,**[‡] **W. Rorer Murphy, Jr., Richard W. Linton, and Thomas J. Meyer***

Contribution from the Department of Chemistry, University of North Carolina, Chapel Hill, North Carolina 27514. Received February 27, 1984

Abstract: The activation of glassy carbon electrodes toward electron-transfer pathways involving proton-coupled electron transfer has been investigated. Oxidative activation of glassy carbon electrodes leads to the catalysis of heterogeneous charge transfer for couples involving catechol (1,2-dihydroxybenzene), $(bpy)_2(H_2O)Ru(OH)^{2+}$(bpy is 2,2'-bipyridine), and $(NH_3)_5Ru(OH)^{2+}$ where there are changes in proton content upon oxidation. X-ray photoelectron spectroscopy has been used to determine the changes induced at the electrode surface by the activation procedure. Comparison of the spectral and electrochemical results with earlier studies on related homogeneous proton-coupled electron-transfer reactions suggests that, although a number of effects may be operative, an important basis for electrode activation may be the appearance of phenolic-like groups on the glassy carbon surface and their subsequent involvement in proton-coupled electron transfer.

Electrochemical investigations using solid electrodes are frequently complicated by effects arising from the nature of the electrode surface. This is particularly true of carbon electrodes, where a variety of different materials are available[1] which are quite sensitive to chemical and electrochemical pretreatment procedures.[2] In fact, the possibility of the deliberate modification of *vitreous* (glassy) carbon or carbon paste electrodes via chemical[3,4] or electrochemical[5-7] activation has been investigated.

Our interest in possible surface activation effects at carbon electrodes arose from the fact that the interconversion of redox

couples like $(bpy)_2(H_2O)Ru^{IV}(O)^{2+}/(bpy)_2(H_2O)Ru^{III}(OH)^{2+}$ [8] or H_2O_2/HO_2 is slow at electrode surfaces, and the heterogeneous charge-transfer characteristics depend upon the electrode material,

† Present address: Chemistry Department, Marshall University, Huntington, W. V. 25701.
‡ Present Address: Department of Physical and Inorganic Chemistry, The University of Adelaide, South Australia 5001, Australia.

(1) J. P. Randin, In "The Encyclopedia of Electrochemistry of the Elements", A. J. Bard, Ed., Marcel Dekker, New York, 1976, p 236–238.
(2) Reference 1, p 12.
(3) J. F. Evans and T. Kuwana, *Anal. Chem.*, **51**, 358 (1979).
(4) J. Zak and T. Kuwana, *J. Am. Chem. Soc.*, **104**, 5515 (1982).
(5) (a) R. C. Engstrom, *Anal. Chem.*, **54**, 2310 (1982); (b) R. C. Engstrom, and V. Strasser *ibid.*, **56**, 136–141 (1984).
(6) M. E. Rice, Z. Galus, and R. N. Adams, *J. Electroanal. Chem.*, **143**, 89 (1983).
(7) M. Brezina and A. Hofmanova, *Collect. Czech. Chem. Commun.*, **38**, 985 (1973).
(8) K. J. Takeuchi, G. J. Samuels, S. W. Gerstein, J. A. Gilbert, and T. J. Meyer, *Inorg. Chem.*, **22**, 1407 (1983).

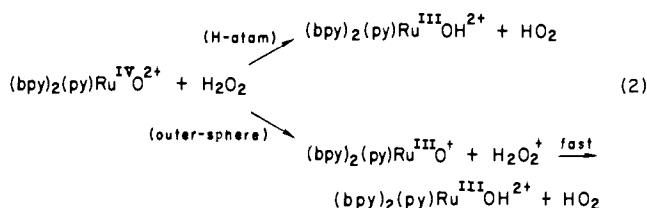the medium, and the conditions used in the electrode pretreatment.[8,10,12-14]

A characteristic feature of such couples is that there is a change in the equilibrium proton content upon oxidation or reduction. In related homogeneous reactions (e.g., eq 1), the electron-transfer

$$(bpy)_2(py)Ru^{IV}O^{2+} + H_2O_2 \rightarrow (bpy)_2(py)Ru^{III}OH^{2+} + HO_2 \tag{1}$$
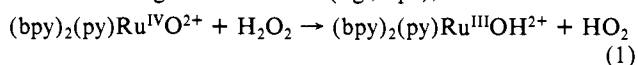
$$k(I = 0.1 \text{ M}, 25.0 \text{ °C}) = 2.1 \text{ M}^{-1} \text{ s}^{-1}; k_{H_2O}/k_{D_2O} = 22$$

(bpy = 2,2'-bipyridine; py = pyridine)

steps involving such couples have been found to be slow and to have unsually large deuterium isotope effects (k_{H_2O}/k_{D_2O}).[9] In this and related reactions,[10,11] it has been suggested that the large isotope effects may signal the intervention of a "proton-coupled" electron transfer or "hydrogen-atom" transfer pathway. Even though mechanistically more complex, such pathways can offer a clear energetic advantage arising from the maintenance of equilibrium proton compositions before and after charge transfer has occurred. In contrast to simple outer-sphere electron transfer, in a proton-coupled electron transfer, the initial products of the redox step are formed in their equilibrium proton structures, e.g., eq 2.

$$(bpy)_2(py)Ru^{IV}O^{2+} + H_2O_2 \quad \begin{array}{c} \xrightarrow{(\text{H-atom})} (bpy)_2(py)Ru^{III}OH^{2+} + HO_2 \\ \\ \xrightarrow{(\text{outer-sphere})} (bpy)_2(py)Ru^{III}O^+ + H_2O_2^+ \xrightarrow{fast} \\ \\ (bpy)_2(py)Ru^{III}OH^{2+} + HO_2 \end{array} \tag{2}$$

In the homogeneous reactions, the H-atom pathway appears to represent a relatively facile mechanism, which takes advantage of the ability of a redox site to act simultaneously as both electron and a proton acceptor. Such pathways might be expected to be of importance for couples involving net proton gains and losses, as in the $(bpy)_2(py)Ru^{IV}(O)^{2+}/(bpy)_2(py)Ru^{III}(OH)^{2+}$ couple shown in eq 1, as well as for some biologically significant couples, such as $NADH/NAD^+$.[15]

The point of the present work was to explore the possibility of creating surface chemical sites at carbon electrode surfaces having the characteristics needed to provide a basis for proton-coupled electron transfer pathways, perhaps similar in detail to the one shown in eq 1.

Experimental Section

Chemicals. The synthesis of $(bpy)_2Ru(CO_3)$,[16] [(terpy)(bpy)Ru-(OH)](ClO_4)_2,[14] and [(NH_3)_5Ru(OH_2)]_2(S_2O_6)_3[17] have been described previously. Catechol (Aldrich Chemical Co.), $K_4Fe(CN)_6$ (J. T. Baker Chemical Co.), 65–70% $HClO_4$ (J. T. Baker Chemical Co.), CF_3COONa (Fisher Scientific Co.), CF_3COOH (Fisher Scientific Co.), $NaClO_4$ (Fisher Scientific Co.), and H_2SO_4 (Mallinckrodt Inc.) were reagent grade and used without further purification. Tris(hydroxymethyl)-aminomethane (THAM), KH_2PO_4, and Na_2HPO_4 were obtained as primary standard grade reagent (Fisher Scientific Co.), and deuterium oxide (Aldrich Chemical Co.) was obtained in 99.8% isotopic purity.

Carbon Electrodes. The vitreous or "glassy" carbon was purchased from Atomergic Chemetals (V10-50) in 3 × 15 mm disks and 3-mm diameter rods. The rods were cut into ca. 1-cm lengths, mounted in a brass holder, and press-fitted into a Teflon (TFE) shroud. The shrouded electrodes were ground flat with 300- and 600-grit carbide paper and

coarse polished with 0000-grit emery paper. The disk and rod electrodes were polished with 1-μm alumina slurried with deionized water and 1-μm diamond paste slurried with diamond paste extender, all on a Microcloth pad with an 8-in. polisher/grinder. All polishing equipment and supplies were obtained from Buehler, Ltd.

Electrode Cleaning. Before each activation experiment, the electrodes were cleaned in the following manner. They were polished with 1-μm alumina suspension for 2 min at high speed, rinsed under a stream of deionized water, then sonicated with a Branson B 22-4 ultrasonic cleaner in a beaker containing deionized water for 30 s (minimum). Both the electrodes and the beaker were then rinsed under a stream of deionized water. The last two steps were repeated. The electrodes were then polished with 1-μm diamond slurry for 2 min at high speed, and the rinsing and sonicating steps were repeated.

Activation Procedure. The electrodes were activated oxidatively in nondegassed 0.1 M H_2SO_4 for various times at an applied potential of +1.80 V.[18] When a reductive step is indicated, the electrodes were held at an applied potential of −0.20 V.

Electrochemical Equipment. Cyclic voltammetry and controlled potential electrolyses were performed with a Princeton Applied Research (PAR) Model 173 potentiostat/galvanostat equipped with a Model 179 digital coulometer. Triangle waveforms for cyclic voltammetry were generated with a PAR Model 175 universal programmer. The current–potential curves were recorded on a Hewlett-Packard Model 7015B x-y recorder with the low pass filters engaged to reject 60-Hz noise. The electrochemical cell consisted of a 30- or 50-mL beaker, a platinum wire auxilary electrode, a glassy carbon working electrode, and a saturated sodium chloride calomel electrode with a cellulose fiber junction. Solution acidity was measured with a Radiometer 62 pH meter with separate glass and calomel electrodes calibrated against standard buffers or acid standards (Fisher Scientific Co.). The platinum working electrode was constructed by silver soldering a platinum button (Englehardt Industries) to a brass mount, press-fitting it into a Teflon (TFE) shroud, followed by the polishing and cleaning procedures described for carbon electrodes. The electrode rotator was a Pine Instruments Model ASRP. The electrodes were rotated at 2000 rpm, with a potential scan rate of 10 mV/s.

Electrochemistry. The voltammetric behaviors of $(NH_3)_5Ru(OH)^{3+}$, o-$C_6H_4(OH)_2$ (catechol), $Fe(CN)_6^{4-}$, $(bpy)_2Ru(OH_2)_2^{2+}$, $(trpy)(bpy)$-$Ru(OH_2)^{2+}$, (trpy = 2,2',2''-terpyridine), H_2O_2, and $(CH_3)_2CHOH$ were investigated in aqueous media. For the electrode activation studies using $(NH_3)_5Ru(OH_2)^{3+}$, $(terpy)(bpy)Ru(OH_2)^{2+}$, $(bpy)_2Ru(OH_2)_2^{2+}$, and $Fe(CN)_6^{4-}$, the pH and/or supporting electrolyte conditions were chosen to yield optimal results. Complex concentrations used were in the range 1.0–5.0 mM. Experiments using the ferrocyanide ion, $Fe(CN)_6^{4-}$, were carried out in 2 M KCl solution, as recommended by Adams.[19] Under these conditions, $Fe(CN)_6^{4-}$ has a diffusion coefficient of 0.750×10^{-5} cm/s and $Fe(CN)_6^{3-}$ a diffusion coefficient of 0.629×10^{-5} cm/s. The pentaamine complex of Ru^{III} as the dithionate salt, $[(NH_3)_5Ru(O-H_2)]_2(S_2O_6)_3$, was studied at various pH values between 7.67 to 10.33. The pH dependence of ΔE_p values (the difference in peak potential for the oxidative and reductive components of a voltammetric wave) was measured in solutions that were 0.2 M in CF_3COONa and 0.05 M in Na_2HPO_4 with CF_3COOH added to adjust acidity. The dependence of ΔE_p on added anion was obtained in solutions that were 0.1 M in THAM with $HClO_4$ added to adjust acidity. The solution in which D_2O and H_2O were compared were of similar compositions, with the D_2O solutions adjusted to be 0.4 pH unit less acidic than H_2O solutions to correct for the activity difference between deuterium and protium ions.[20] The deuterium isotopic purity was 90% in solutions used to check deuterium isotope effects. Solutions containing the ion $(bpy)_2Ru(OH_2)_2^{2+}$ were prepared by dissolving the complex $(bpy)_2Ru(CO_3)$ in 0.1 M $HClO_4$ which gives $(bpy)_2Ru(OH_2)_2^{2+}$ with loss of CO_2. This solution was added to 0.2 M KH_2PO_4 until the pH was 2.46. Solutions containing the ion $[(trpy)(bpy)Ru(OH_2)](ClO_4)_2$ were made with pH 6.86 buffer (Fisher Scientific Co.). Electrochemical experiments based on hydrogen peroxide, isopropyl alcohol, and catechol were performed in 0.1 M H_2SO_4.

The ΔE_p values from cyclic voltammograms were used as a qualitative measure of changes in reversibility, since in most cases they were too large to permit the calculation of the heterogeneous charge-transfer rate constant using the treatment of Nicholson.[21] The decreases in the ΔE_p values with activation provide qualitative evidence for a corresponding

(9) J. A. Gilbert, S. W. Gersten, and T. J. Meyer, *J. Am. Chem. Soc.*, **104**, 6872 (1982).

(10) B. A. Moyer and T. J. Meyer, *Inorg. Chem.*, **20**, 436 (1981).

(11) R. A. Binstead, B. A. Moyer, G. J. Samuels, and T. J. Meyer, *J. Am. Chem. Soc.*, **103**, 6872 (1982).

(12) J. M. Calvert and T. J. Meyer, *Inorg. Chem.*, **21**, 3978 (1982).

(13) K. J. Takeuchi, S. W. Gersten, G. J. Samuels, J. A. Gilbert, and T. J. Meyer, in preparation.

(14) K. J. Takeuchi, D. Pipes, M. S. Thompson, and T. J. Meyer, *Inorg. Chem.*, **23**, 1845 (1984).

(15) W. J. Blaedel and R. A. Jenkins, *Anal. Chem.*, **47**, 1337 (1973).

(16) E. C. Johnson, B. P. Sullivan, D. J. Salmon, and T. J. Meyer, *Inorg. Chem.*, **17**, 2211 (1978).

(17) A. A. Diamantis, W. R. Murphy, Jr., and T. J. Meyer, *Inorg. Chem.*, **23**, 3230 (1984).

(18) All potentials are reported vs. the saturated sodium chloride calomel electrode, which is +0.236 V with respect to the normal hydrogen electrode (see A. J. Bard and L. R. Faulkner, "Electrochemical Methods", Wiley, New York, 1980, end pages).

(19) R. N. Adams, "Electrochemistry at Solid Electrodes", Marcel Dekker, New York, 1969, p 223.

(20) R. G. Bates, "Determination of pH", Wiley, New York, 1964, p 220.

(21) R. S. Nicholson, *Anal. Chem.*, **37**, 1351 (1965).

Table I. Surface and Subsurface Compositions of Glassy Carbon Electrodes (by X-ray PES)[a]

element (photo-electron)	without activation		oxidation only		oxidation followed by reduction	
	surface	sub-surface	surface	sub-surface	surface	sub-surface
Al (2p)	ND	ND	ND	ND	ND	ND
C (1s)	81	98	65	97	72	96
Cl (2p)	ND	0.2	0.9	0.6	0.9	0.3
N (1s)	1.7	ND	0.7	ND	ND	ND
O (1s)	15	1.9	32	1.4	23	2.9
Si (2p)	2.4	ND	0.5	ND	2.8	0.9
S (2p)	0.3	ND	1.1	0.8	0.4	ND

[a] Empirical elemental sensitivity factor method used. Detectable elements normalized to 100% atomic. ND means not detected.

increase in the heterogeneous charge-transfer rate constants. For some cases there are large uncertainties associated with the ΔE_p values due to the broadness of the waves obtained at unactivated electrodes. Such values are labeled with an asterisk (*).

It should be noted that under our conditions uncompensated cell resistance appears to be negligible as shown by experiments using couples where kinetic effects are small. For example, at activated electrodes, ΔE_p reaches the expected value of 59 mV at scan rates below 100 mV/s for the $Fe(CN)_6^{3-/4-}$ and $Ru(trpy)(bpy)OH^{2+}/Ru(trpy)(bpy)OH_2^{2+}$ couples.

X-ray Photoelectron Spectroscopy (X-ray PES). Changes in the surface composition of the glassy carbon electrodes as a result of activation were monitored by X-ray PES. In preparation for X-ray PES analysis, the disks were polished and treated as described above. To prepare "oxidized" disks, polished disks were held at an applied potential of +1.80 V for 30 min after polishing was complete. To prepare reduced disks, oxidized disks were prepared as above, followed by reduction at an applied potential of -0.20 V for 5 min. The oxidized and the oxidized-reduced electrodes were removed from the solution while still at the appropriate applied potential and rinsed with distilled water.

All spectra were collected at residual gas pressures less than 7×10^{-9} torr using a Perkin-Elmer Physical Electronics Model X-ray PES/Auger electron spectrometer equipped with a magnesium anode X-ray source and double-pass cylindrical mirror analyzer. Spectral coaddition, $K\alpha$ satellite removal, and subsequent data processing were performed using a locally constructed Intel Z80 based microcomputer and associated software.[22,23] After the initial analysis, each electrode was subjected to Ar^+ sputtering in the spectrometer (Kratos Minibeam I ion gun) so that interior and surface compositions could be compared using X-ray PES. Argon ions (4.5 kV, 2 μA/cm² current density) were used to etch each disk for 25 min. Under identical conditions (Ar partial pressure, time, acceleration voltage, and filament emission current of 15 mA) the gun removed 0.8 nm/min of SiO_2 from the surface of a silicon wafer as measured by ellipsometry.

Results

Activated Electrodes. The appearance of the electrode surface at each stage of the activation procedure was distinctive. Freshly polished electrodes are black, lustrous and mirror-like, and bead water, suggesting the presence of hydrophobic groups on the surface. In the initial stages of the oxidative treatment, the surface appears to be metallic green, followed by a purple-gold and then a golden hue as oxidation time is increased. The oxidized layer is more brittle than the bulk of the electrode and can be scratched by gentle abrasion and beads of water. The same observation has been made by Engstrom and Strasser.[5b] Electrodes which were oxidized and then reduced have a dull golden surface which wets with water, suggesting the presence of hydrophilic groups on the surface. Surface analysis data for polished and activated electrodes appear in Table I as do data on bulk composition obtained by Ar^+ sputtering. Some points to emerge from the data include: (1) the absence of detectable metals, including the fact that the surface concentration of aluminum is below the X-ray PES (1.5% atomic) and Auger (<0.25%) limits[24] of detection [as a consequence, we
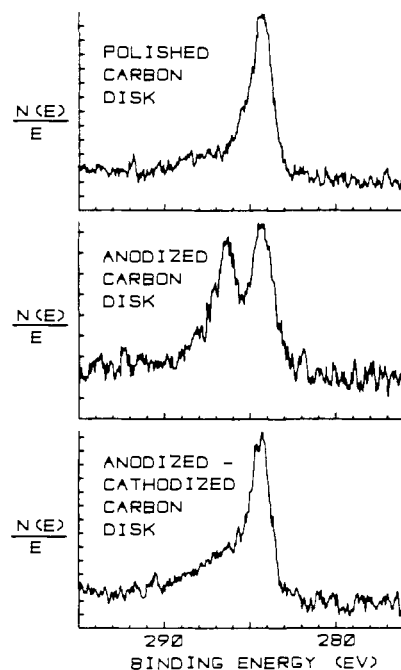
Figure 1. X-ray PES high-resolution spectra of glassy carbon disks as a function of electrochemical pretreatment (see text).

Table II. Carbon (1s) Binding Energies of Oxygen-Containing Functional Groups[a]

functional group	lit. value[27] (eV)	value obtained from curve fits (eV)	from d^2x/dE^2 (eV)
graphitic (tetrahedral)	284.3 ± 0.1	284.3	284.3 ± 0.2
alcoholic (phenolic)	286.1 ± 0.1	286.2	286.2 ± 0.2
carbonyl	287.7 ± 0.1	287.7	287.2 ± 0.2
carboxylic acid	289.1 ± 0.1	289.1	ND

[a] All binding energies were corrected for sample charging assuming graphitic carbon = 284.3 eV. ND means not detected.

conclude that the basis for electrode activation observed here is not related to the effect observed by Zak and Kuwana,[4] where high (30%) surface coverages of aluminum were reported resulting from intentional incomplete cleaning of the polishing medium (alumina) from the electrodes]; (2) the presence of only trace concentrations of chlorine and surfur, as chloride and sulfate, due to adsorption of SO_4^{2-} from the electrolyte solution (0.1 M H_2SO_4) and Cl^- from the SSCE reference electrode leakage;[25] (3) most importantly, an increase in the surface oxygen content by a factor of 2 with respect to untreated electrodes with a corresponding decrease in the carbon concentration. The subsequent reduction step removes only part of the oxygen introduced in the oxidation step.

High resolution carbon (1s) spectra of untreated, oxidized, and oxidized-reduced disks appear in Figure 1. Because of the buildup of oxygen on the surface as a consequence of oxidation, the enhancement in the high binding energy components of the carbon (1s) photoelectron line upon oxidation can be associated with the formation of oxygen-containing functional groups on the surface. A number of groups have been suggested[26] including carboxylic acids, acid anhydrides, alcohols, phenols, ketones, and quinones. Table II lists both representative functional groups and their approximate C(1s) binding energies.[27] From the spectra in Figure 2 (see below), it would appear that the major resolvable types of

(22) F. E. Woodard, W. S. Woodward, and C. N. Reilley, *Anal. Chem.*, **53**, 1251A (1981).

(23) D. F. Smith, Ph.D. Dissertation, University of North Carolina, 1978.

(24) L. E. Davis, N. C. MacDonald, P. W. Palmberg, G. E. Riach, and R. E. Weber, "Handbook of Auger Electron Spectroscopy", 2nd ed., Physical Electronic Industries, Inc., Eden Prairie, Minn., p 13.

(25) D. T. Sawyer and J. L. Roberts, Jr., "Experimental Electrochemistry for Chemists", Wiley, New York, 1974.

(26) J. P. Randin in ref 1, pp 23 and 27.

(27) C. D. Wagner, W. M. Riggs, L. E. Davis, J. F. Moulder, and G. E. Muilenburg, "Handbook of X-Ray Photoelectron Spectroscopy", Perkin Elmer Corp., Physical Electronics Div., Eden Prairie, Minn.
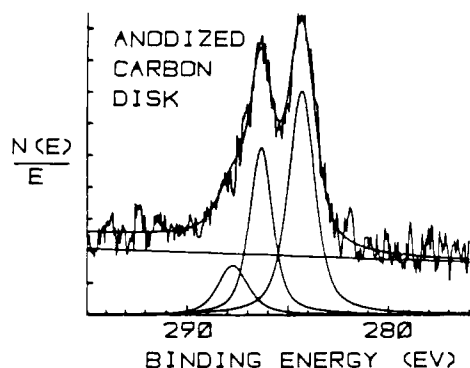
Figure 2. An example of the results obtained by the X-ray PES curve-fitting algorithm (see Table III for quantitative results).

Table III. Relative Surface Concentration of Different Carbon Functional Groups (as Percentage of Carbon Atoms Detected)

function group type[a]	unac-tivated	oxidatively activated	oxidatively and reductively activated
1. graphitic	76	53	65
2. phenol, alcohol, ether	15	34	21
3. ketone, quinone, aldehyde	5	13	9
4. carboxylate,[b] acid anhydride	5	<1	4
oxidized C/graphitic C[c]	0.19	0.49	0.32
O/C atomic ratio[d]	0.33	0.89	0.52
(oxidized C/graphitic C)/ (O/C atomic ratio)	1.7	1.8	1.6

[a] As estimated using the curve-fitting procedure. [b] The uncertainties in the carboxylate–acid anhydride numbers may be significant due to interference from a surface plasmon loss at 291.2 eV (Proctor, A.; Sherwood, P. M. A. *Carbon* **1983**, *21*, 53–59) which obviates the possibility of making detailed comparisons. [c] Oxidized carbon includes the integrated sum of all of the oxidized functional groups (2–4). [d] See Table I.

oxygen containing surface groups formed during the surface oxidation step are either alcohol or ether groups. Contributions from carbon in the higher formal oxidation states associated with carbonyl or carboxylate groups appear in the high binding energy tail and are present at lower surface concentrations. At first glance, our conclusions are at odds with results obtained earlier using attenuated total reflectance infrared spectroscopy,[28,29] which suggested that the principal surface groups are carbonyl containing. However, it should be realized that, although roughly the same sensitivity exists for all carbon containing groups in X-ray PES analysis, the infrared analysis will necessarily favor carbonyl groups because of their relatively high absorption coefficients.

An iterative spectral curve-fitting routine designed for X-ray PES applications[23] was used to estimate the relative concentrations of the various carbon-containing components in the three types of disks. In the fits it was assumed that the peak widths as full widths at half-maximum (fwhm) were between 1.3 and 1.9 eV. The fwhm of the carbon (1s) peak of the polished electrode is 1.5 eV (Figure 1). In the fit it was assumed that carbon was present as (1) graphitic or tetrahedral carbon, (2) carbon adjacent to oxygen in an alcohol, phenol, or ether, (3) carbonyl carbon in an aldehyde, ketone, or quinone, or (4) carbon in a carboxylic acid or anhydride. An example of a result of the fitting procedure is illustrated in Figure 2, and the carbon surface compositions for the three electrode surfaces obtained by the fitting procedure are summarized in Table III. Since the number of unknowns exceed the number of equations used in the fitting procedure, the compositions generated by the curve-fitting procedures are not unique. However, the percentages calculated in several independent trials varied only a few percent from those listed (note Chapters 5 and
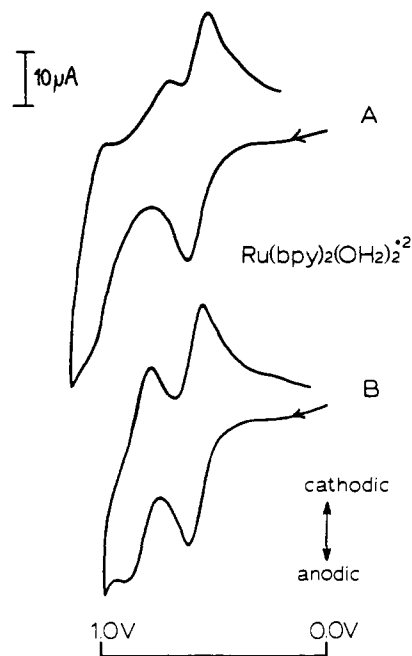
(28) J. S. Mattson and H. B. Mark, Jr., *Anal. Chem.*, **41**, 355 (1969).
(29) J. S. Mattson and H. B. Mark, Jr., *J. Colloid Interface Sci.*, **31**, 131 (1969).

Figure 3. Cyclic voltammograms for $(bpy)_2Ru(OH)_2^{2+}$ in a pH 2.5 buffer solution ($HClO_4$ and KH_2PO_4) at untreated (A) and activated (B) glassy carbon electrodes. The activation procedure consisted of three sequences of potential holding at +1.80 V for 30 s followed by 15 s at −0.20 V in 0.1 M H_2SO_4. Scan rate is 20 mV/s.

7 in ref 30). The qualitative validity of the fitting procedure is substantiated by the data in Table III where it can be seen that O/C atomic ratios and the oxidized C graphitic C ratios parallel each other as expected. The two ratios are not expected to be identical for a given electrode because of the different carbon/oxygen ratios associated with different functional groups, e.g., ethers and alcohols. The validity of the curve-fitting results is supported by second-derivative X-ray PES spectra, as shown in Table II, and reported in detail in ref 30. It should be noted that similar X-ray PES results have been reported by Engstrom and Strasser, but that they made no attempt to treat their data by curve fitting.[5b]

Given the electrocatalytic properties of the activated electrodes discussed below and the nature of the activation process, it is important to establish whether or not the activation procedure results in an increase in the effective surface area of the electrode. The surface area of an electrode before and after activation (oxidation activation at +1.8 V for 5 min, in 0.1 M H_2SO_4) was determined by chronoamperometry using the $Fe(CN)_6^{4-/3-}$ couple. The experiments were carried out in a solution of $K_4Fe(CN)_6$ (4.28 mM) in 2 M KCl by stepping the potential from 0.0 V to the diffusion plateau for the $Fe(CN)_6^{4-/3-}$ wave (0.50 V). For the unactivated electrode, 17 data points were taken from t = 3.6 to 4.6 s giving an average value of 0.083 ± 0.002 cm^2. For the activated electrode the area was 0.078 ± 0.001 cm^2. It should be noted that this experiment shows only that there is no *gross* change in electrode geometry during the activation procedure. The *microscopic* surface area could be considerable different after the activation procedure.

Electrochemistry. Table IV shows the decrease in ΔE_p values for the redox couples of catechol, $Ru(NH_3)_5(OH_2)^{3+}$, and $Ru(bpy)_2(OH_2)_2^{2+}$ as the electrode was activated by oxidation alone (for catechol) or by sequences of oxidation (30 s) followed by reduction (15 s) for the metal complexes. In each case, an increase in the duration of the oxidative treatment results in a decrease in ΔE_p. As noted earlier by Engstrom in a related study,[5] for our metal complex studies we found it necessary to follow the oxidative step with a short reductive step in order to minimize ΔE_p.

(30) G. E. Cabaniss, Ph.D. Dissertation, University of North Carolina at Chapel Hill, 1984.

Table IV. Results of Electrode Activation[a]

couple A		couple B		couple C		
activation	$n\Delta E_p$ (mV)	activation	$n\Delta E_p$ (mV)	activation	$n\Delta E_p$ (mV)	k_s (cm/s)
none	610	none	890	none	>200	$>5 \times 10^{-4}$
1×	380	120 s	770	1×	150	$1.11 \pm 0.06 \times 10^{-5}$
2×	260	720 s	570	2×	140	$1.1 \pm 0.2 \times 10^{-3}$
3×	190	1680 s	190	4×	110	$2.1 \pm 0.2 \times 10^{-3}$
				6×	120	$1.9 \pm 0.2 \times 10^{-3}$

couple A: $[(NH_3)_5Ru^{IV}(O)]^{2+} + H^+ + e^- \rightleftharpoons [(NH_3)_5Ru^{III}(OH)]^{2+}$
the medium is 0.1 M NaClO$_4$, 0.1 M THAM, and HClO$_4$ (70%) to pH 8.7; scan rate is 100 mV/s; $n = 1$

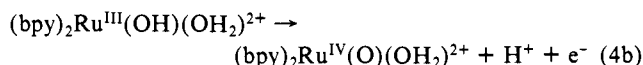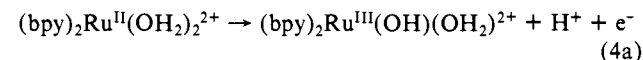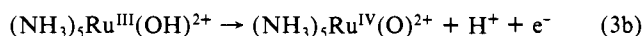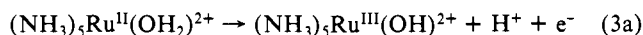couple B: $+ 2H^+ + 2e^- \rightleftharpoons$
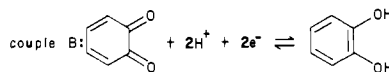
the medium is 0.1 M H$_2$SO$_4$; scan rate is 100 mV/s; $n = 2$

couple C: $[(bpy)_2Ru^{IV}(OH_2)(O)]^{2+} + H^+ + e^- \rightleftharpoons [(bpy)_2Ru^{III}(OH_2)(OH)]^{2+}$
the medium is 0.2 M KH$_2$PO$_4$ and HClO$_4$ (70%) until the pH was 2.46; $n = 1$; scan rate is 20 mV/s

[a] Activation for couples A and C consisted of cycles of oxidation of the electrode for 30 s at +1.80 V, followed by a reductive treatment for 15 s at −0.20 V, all in 0.1 M H$_2$SO$_4$. × refers to one such cycle. Activation for couple B consisted of seconds of an oxidative treatment of the electrode at +1.80 V in 0.1 M H$_2$SO$_4$. No reductive treatment was used for couple B.

For the metal complexes, the pH conditions were such that a single proton change is associated with the couples, eq 3 and 4.

$$(NH_3)_5Ru^{II}(OH_2)^{2+} \rightarrow (NH_3)_5Ru^{III}(OH)^{2+} + H^+ + e^- \quad (3a)$$

$$(NH_3)_5Ru^{III}(OH)^{2+} \rightarrow (NH_3)_5Ru^{IV}(O)^{2+} + H^+ + e^- \quad (3b)$$

$$(bpy)_2Ru^{II}(OH_2)_2^{2+} \rightarrow (bpy)_2Ru^{III}(OH)(OH_2)^{2+} + H^+ + e^- \quad (4a)$$

$$(bpy)_2Ru^{III}(OH)(OH_2)^{2+} \rightarrow$$
$$(bpy)_2Ru^{IV}(O)(OH_2)^{2+} + H^+ + e^- \quad (4b)$$

The effects of electrode activation on the Ru(IV)/Ru(III) and Ru(III)/Ru(II) couples of $(bpy)_2Ru(OH_2)_2^{2+}$ are shown in Figure 3. At more oxidizing potentials additional waves are observed for the Ru(VI)/Ru(V) $[(bpy)_2Ru(O)_2^{2+}/(bpy)_2Ru(O)(OH)^{2+}]$ and Ru(V)/Ru(IV) $[(bpy)_2Ru(O)(OH)^{2+}/(bpy)_2Ru(O)(OH_2)^{2+}]$ couples.[8] In fact, because of the slow charge-transfer rate at an unactivated electrode, the oxidative component of the Ru(IV)/Ru(III) wave is shifted sufficiently far positively that it overlaps with the oxidative component of the Ru(V)/Ru(IV) wave.

The voltammograms in Figure 3 show that the wave for the Ru(IV)/Ru(III) couple is highly susceptibile toward electrode activation, ultimately becoming a well-resolved, quasi-reversible wave with $\Delta E_p = 212$ mV and $k_s = 2.3 \times 10^{-3}$ cm/s, while the Ru(III)/Ru(II) wave is quasi-reversible even at a polished electrode. For the Ru(IV)/Ru(III) couple, variations in k_s and ΔE_p as a function of the number of activation cycles are summarized in Table IV. It is notable that on the sixth cycle of activation, an actual decrease in k_s is observed.

Electrochemical data for the various couples are summarized in Tables IV and V. Note that from the data for the Ru-(IV)/Ru(III) and Ru(III)/Ru(II) couples, ΔE_p is dependent on sweep rate, and the ratio $i_p/\nu^{1/2}$ decreases with increasing sweep rate. Both of these observations are consistent with less than diffusion-controlled charge transfer to and from the electrode.[31]

For purposes of comparison, cyclic voltammograms for the related Ru(IV)/(III) and Ru(III)/(II) couples [(trpy)(bpy)Ru-(O)$^{2+}$/(trpy)(bpy)Ru(OH)$^{2+}$] and [(trpy)(bpy)Ru(OH)$^{2+}$/(trpy)(bpy)Ru(OH$_2$)$^{2+}$] are shown in Figure 4. Note that the response to electrode activation by the Ru(IV)/(III) couple is in marked contrast to the response of the (bpy)$_2$Ru(OH$_2$)$_2^{2+}$-based Ru(IV)/(III) couple. For the trpy couple, electrode activation leaves ΔE_p unaffected, but the peak currents associated with the Ru(IV)/(III) couple are noticeably enhanced.

Equally dramatic increases in the heterogeneous charge-transfer rate for the (NH$_3$)$_5$Ru(O)$^{2+}$/(NH$_3$)$_5$Ru(OH)$^{2+}$ couple occur upon electrode activation, as shown in Figure 5 and by the data in Tables

(31) A. J. Bard and L. R. Faulkner, "Electrochemical Methods", Wiley, New York, 1975, pp 290–291.

Table V. Sweep Rate Dependence of Peak Currents and ΔE_p Values

couple	ν (mv/s)	i_p (mA)	$i_p/\nu^{1/2}$	ΔE_p (mV)
(bpy)$_2$Ru^{III}(OH)(OH$_2$)$^{2+}$/	200	56	3.9	110
(bpy)$_2$Ru^{II}(OH$_2$)$_2^{2+}$[a]	100	44	4.4	95
	50	34	4.8	90
	20	24	5.3	80
(bpy)$_2$Ru^{IV}(O)(OH$_2$)$^{2+}$/	200	41	2.9	270
(bpy)$_2$Ru^{III}(OH)(OH$_2$)$^{2+}$[a]	100	29	2.9	220
	50	21	3.0	190
	20	14	3.1	170
(NH$_3$)$_5$Ru^{III}(OH)$^{2+}$/	200	50	3.5	100
(NH$_3$)$_5$Ru^{II}(OH$_2$)$^{2+}$[b]	100	27	2.7	95
	50	18	2.6	85
	20	11	2.5	75
(NH$_3$)$_5$Ru^{IV}(O)$^{2+}$/	200	41	2.9	720
(NH$_3$)$_5$Ru^{III}(OH)$^{2+}$[b]	100	27	2.7	660
	50	18	2.6	590
	20	11	2.5	
catechol[c]	200	314	22	
	100	231	23	
	50	167	24	
	20	110	25	
	10	81	25	

[a] Activated electrode (2 × 30 s oxidative cycles followed by a 15-s reductive cycle) at pH 2.46. For the Ru(III)/(II) couple $k_s = (6.9 \pm 0.6) \times 10^{-3}$ cm/s from the ΔE_p values;[21] i_p^c for Ru(III)/(II) and i_p^a for Ru(IV)/(III) are the data cited. [b] Polished electrode, pH 7.8. For the Ru$^{III/II}$ couple, $k_s = (8.4 \pm 0.7) \times 10^{-3}$ cm/s from the ΔE_p values;[21] i_p^c for Ru(III)/(II) and i_p^a for Ru(IV)/(III) are the data cited. [c] Polished electrode in 0.1 M H$_2$SO$_4$. Note that under these conditions the electrochemical response appears to be that of an irreversible two-electron couple (Figure 6).

Table VI. Anion and H$_2$O/D$_2$O Dependences for the (NH$_3$)$_5$Ru(OH)$^{2+}$/(NH$_3$)$_5$Ru(O)$^{2+}$ Couple at Polished and Activated Electrodes (scan rate = 200 mV/s)

electrode condition	ΔE_p (mV)					
	ClO$_4^-$ [a]	CF$_3$COO$^-$ [a,b]	BF$_4^-$ [a,b]	F$^-$ [a,b]	H$_2$O[c]	D$_2$O[c]
polished	770	770*	850*	770*	720	880
activated	300	190	240	200	270	440

[a] 0.1 M NaX (X = ClO$_4$, BF$_4$, CF$_3$COO$^-$, F$^-$) and 0.1 M THAM with enough HX added to adjust the pH to 8.3; solutions ca. 2 × 10^{-3} M in (NH$_3$)$_5$Ru(OH)$^{2+}$; activation consisted of three cycles of oxidation/reduction as in Table IV, footnote d. [b] The values with asterisks are approximate owing to the broadness of the waves. [c] 0.1 M NaClO$_4$ and 0.1 M THAM with enough HClO$_4$ added to reach pH 7.8 (H$_2$O) or 8.2 (D$_2$O). The D$_2$O was 90% D. The activation procedure consisted of two cycles of oxidation/reduction as in Table IV.

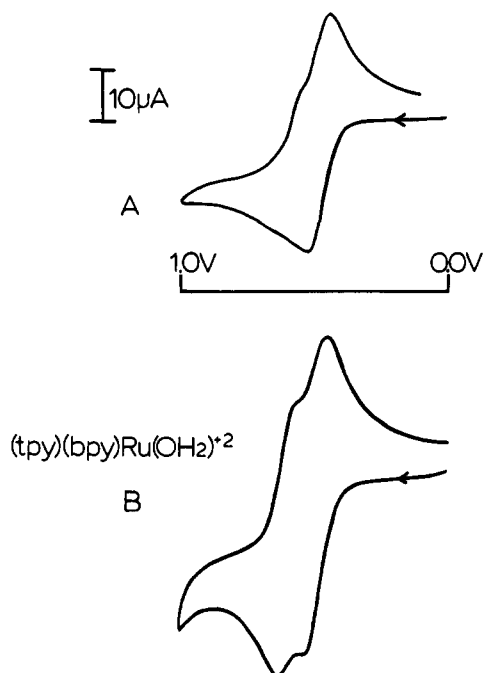IV and V. There is also clear evidence for significant H$_2$O/D$_2$O kinetic isotope effects (Table VI). Before activation, the Ru-

Figure 4. Cyclic voltammograms of $(trpy)(bpy)Ru(OH_2)^{2+}$ in pH 6.86 buffer at glassy carbon electrodes: (A) polished; (B) activated by three cycles of 30 s at 1.80 V and 15 s at −0.20 in 0.1 M H_2SO_4. Scan rate is 20 mV/s.
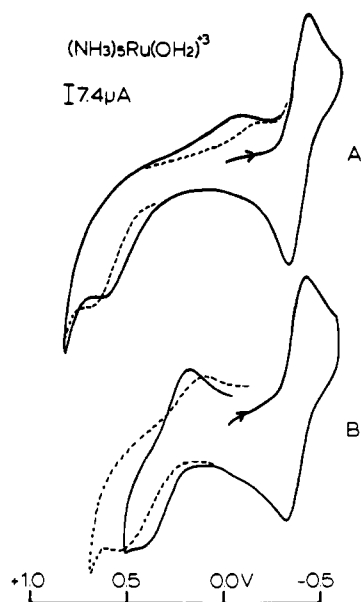

Figure 5. Cyclic voltammograms of $(NH_3)_5Ru(OH)^{2+}$ in H_2O and D_2O at untreated (A) and activated (B) glassy carbon electrodes. The solutions are 0.1 M in $NaClO_4$ and 0.1 M in THAM with 60% $HClO_4$ added until the pH is 7.8 (H_2O,—) or 8.2 (D_2O,---). The activation procedure involved two oxidative sequences of 30 s at +1.80 V, followed by reduction for 15 s at −0.20 V in 0.1 M H_2SO_4. The scan rate is 200 mV/s.

(IV)/(III) couple is electrochemically irreversible in H_2O and even more so in D_2O. Activation of the electrode through three sequences of oxidation–reduction cycles results in a quasi-reversible Ru(IV)/(III) wave with $k_s^{H_2O} = 1.6 \times 10^{-3}$ cm/s. It is not possible to obtain k_s in D_2O since ΔE_p exceeds the maximum value of ΔE_p = 212 mV defining the limit of validity of the treatment. Using $\Delta E_p(D_2O) = 212$ mV gives for a minimum deuterium kinetic isotope effect $k_s^{H_2O}/k_s^{D_2O} > 3.2$. The existence of significant anion effects on ΔE_p for the $(NH_3)_5Ru(O)^{2+}/(NH_3)_5Ru(OH)^{2+}$ couple is also shown by the data in Table VI.

For the $Fe(CN)_6^{3-/4-}$ couple in 2 M KCl, electrode activation (5 min of oxidation and 15 s of reduction) also leads to an increase in k_s and to a measurable kinetic isotope effect at least for the

Table VII. k_s Dependence for $K_4Fe(CN)_6$ in 2 M KCl on Electrode Activation and Solution Isotopic Composition

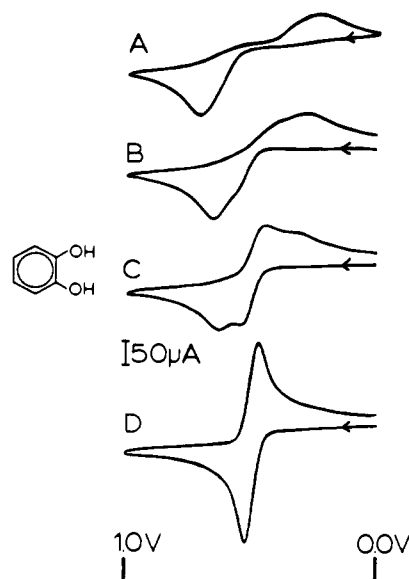| activation	$\Delta E_p^{H_2O}$ (mV)	$k_s^{H_2O}$ (cm/s)	$\Delta E_p^{D_2O}$ (mV)	$k_s^{H_2O}$ (cm/s)	$k_s^{H_2O}/k_s^{D_2O}$
polished	88	8×10^{-3}	130	3×10^{-3}	2.7
activated	65	5×10^{-2}	67	3×10^{-2}	1.4

Figure 6. Cyclic voltammograms of catechol (8 mM) in 0.1 M H_2SO_4 for electrode activation periods of 0 min (A), 2 min (B), 12 min (C), and 28 min (D). The scan rate is 100 mV/s.

polished electrode as shown by the data in Table VII.

Figure 6 shows a series of cyclic voltammograms for the oxidation of catechol. At a polished electrode (Figure 6A), an oxidation and its associated reduction appear, but the two peak potentials are widely separated, the waves are broad, and the peak currents are unequal. After partial electrode activation, two distinct components appear in both the oxidative and reductive waves which correspond to two, one-electron components of the overall two-electron process:
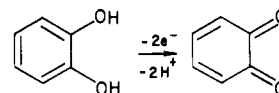
In the early stages of electrode activation, the wave for the initial oxidation step:
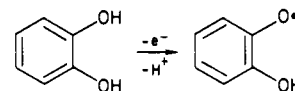
is selectively catalyzed and approaches the wave characteristics expected for a reversible, one-electron couple.[31] Past this point the couple is nearly diffusion controlled and further electrode activation has no effect. However, with further activation, the second, one-electron oxidation:
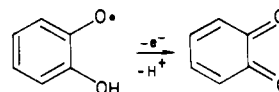
is catalyzed further and eventually overtakes the first wave. At the fully activated electrode, the wave shape approaches that expected for an overall two-electron process where the intermediate oxidation state is unstable with respect to disproportionation, and the electrode processes involved are kinetically facile.[31]

The quinone product of the two-electron oxidation of catechol is stable on the cyclic voltammetric time scale, but on longer time scales undergoes a 1,4 addition to give 1,2,4-trihydroxybenzene as the ultimate product.

The electrochemistry of catechol is complicated by adsorption of catechol and/or its oxidation products,[32] but it is to be emphasized that the observations made here pertain to activation of the electrode toward the solution couples. The same results were obtained for initial cyclic scans, where adsorption is minimal, and for later scans, where noticeable adsorption had occurred. The extent of adsorption can be monitored by the appearance of a surface wave at $E_{1/2} = 0.50$ V when the potential of a polished electrode is cycled between 0 and 1.0 V. The wave characteristics of the surface wave at $E_{1/2} = 0.50$ V are closely related to those obtained for catechol in solution and the wave is probably attributable to adsorbed catechol. More complex patterns of surface waves can not be obtained by potentiostatting electrodes at more positive potentials in the presence of catechol.[32]

In 0.1 M H_2SO_4 containing 2×10^{-3} M $(CH_3)_2CHOH$, no oxidation waves were observed from 0.0 to +1.4 V by rotating disk voltammetry at either polished or activated (30 min at +1.80 V in 0.1 M H_2SO_4) electrodes. Similarly, no significant current enhancement (<0.18 M A/cm^2 over background was observed for solutions containing 2×10^{-3} M H_2O_2 at a polished electrode. By contrast, oxidative activation of a carbon electrode (5 min at +1.80 V in 0.1 M H_2SO_4) results in a marked increase in current density for the oxidation of H_2O_2 (340 mA/cm^2 over a background current density of 7.1 mA/cm^2 at 1.35 V). In D_2O (0.1 M D_2SO_4) an increase of only 2.7 mA/cm^2 was observed at the same potential ($j_{H_2O} = 130 j_{D_2O}$). Although difficult to evaluate quantitatively because of the absence of a well-defined waveshape, it is obvious that oxidative activation has a *profound* effect on the ability of the electrode to oxidize H_2O_2 and that the pathway created by oxidative activation is subject to a dramatic H/D kinetic isotope effect.

Discussion

In order to develop a reasonable model for the origin of the electrode activation effects, the related homogeneous redox reactions should first be considered. As a class, polypyridyl complexes of ruthenium characteristically undergo facile electron transfer, as evidenced by the large self-exchange rate constants for $(bpy)_3Ru^{3+/2+}$ and related couples which are close to the diffusion-controlled limit.[33] Such complexes also undergo facile heterogeneous electron transfer at a variety of electrode materials (Pt, Au, glassy carbon, and carbon paste) in several solvents.[34] Such observations show that the electronic coupling factors and vibrational barriers to electron transfer for this class of molecules are normally low, and, as a consequence, their electron-transfer reactions are rapid.[33b,35]

For the Ru(IV)/(III) couple, $(bpy)_2(py)Ru^{IV}(O)^{2+}/(bpy)_2$-$(py)Ru^{III}(OH)^{2+}$ or, below pH 2, $(bpy)_2(py)Ru^{IV}(O)^{2+}/(bpy)_2$-$(py)Ru^{III}(OH_2)^{3+}$, oxidation of Ru(III) to Ru(IV) involves a loss of protons.[10] Simple outer-sphere oxidation of Ru(III) would necessarily lead to a Ru(IV) site which is initially not at equilibrium with regard to proton content:

$$(bpy)_2(py)Ru^{III}(OH)^{2+} \xrightarrow{-e^-} (bpy)_2(py)Ru^{IV}(OH)^{3+} \xrightarrow[fast]{-H^+}$$
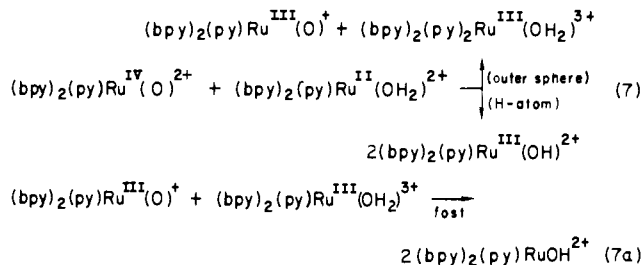$$(bpy)_2(py)Ru^{IV}(O)^{2+} \quad (5)$$
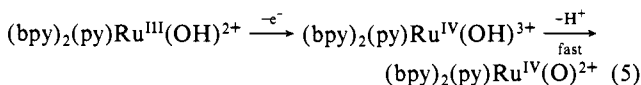
For such a pathway, there is unavoidably a contribution to the free energy of activation arising from the nonequilibrium protonation of the initial Ru(IV) product:

$$(bpy)_2(py)Ru^{IV}(O)^{2+} + H^+ \underset{\rightleftharpoons}{\overset{K_b}{}} (bpy)_2(py)Ru^{IV}(OH)^{3+}$$
$$\Delta G = -RT \ln K_b \quad (6)$$
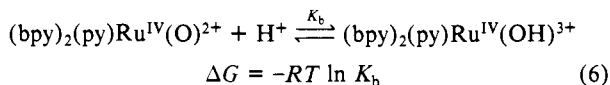
in addition to the usual vibrational and electronic factors associated with electron transfer.

(32) W. R. Murphy, Jr., Ph.D. Dissertation, University of North Carolina at Chapel Hill, 1984.
(33) (a) R. C. Young, F. R. Keene, and T. J. Meyer, *J. Am. Chem. Soc.*, **99**, 2468 (1977). (b) N. Sutin *Prog. Inorg. Chem.*, **30**, 441 (1983). (c) M. S. Chan and A. C. Wahl, *J. Phys. Chem.*, **82**, 2542 (1978). (d) M. W. Dietrich, and A. C. Wahl *J. Chem. Phys.*, **38**, 1591 (1963).
(34) T. Saji and S. Aoyagui, *J. Electroanal. Chem.*, **63**, 31 (1975).
(35) G. M. Brown and N. Sutin, *J. Am. Chem. Soc.*, **101**, 883 (1979).

Evidence for the importance of such effects has been obtained from kinetics studies. For example, the comproportionation reaction in eq 7 has a driving force of -0.11 V and yet the reaction is relatively slow, $k(25 \,^\circ C) = 2.1 \times 10^5$ M^{-1} s^{-1},[11] for this class of reactions. Of the two pathways in eq 7, the outer-sphere

$$(bpy)_2(py)Ru^{III}(O)^+ + (bpy)_2(py)_2Ru^{III}(OH_2)^{3+}$$

$$(bpy)_2(py)Ru^{IV}(O)^{2+} + (bpy)_2(py)Ru^{II}(OH_2)^{2+} \underset{(H-atom)}{\overset{(outer\ sphere)}{\longrightarrow}} \quad (7)$$

$$2(bpy)_2(py)Ru^{III}(OH)^{2+}$$

$$(bpy)_2(py)Ru^{III}(O)^+ + (bpy)_2(py)Ru^{III}(OH_2)^{3+} \xrightarrow{fast}$$
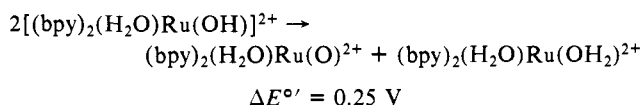
$$2(bpy)_2(py)RuOH^{2+} \quad (7a)$$

pathway followed by rapid proton transfer (eq 7a) can be ruled out since the minimum free energy of activation ($\Delta G^\ddagger$) calculated from the pK_a values for $(bpy)_2(py)Ru^{III}(OH_2)^{3+}$ and $(bpy)_2$-$(py)Ru^{III}(OH)^{2+}$ (0.85 and >13, respectively)[10] is greater than the experimental value. Rather, as evidenced by a k_{H_2O}/k_{D_2O} ratio of 16.1, the reaction appears to occur by a new pathway involving proton-coupled electron (H-atom) transfer. Such pathways avoid the dilemma of forming high-energy intermediates with regard to proton composition, but at the expense of mechanistic complexity. In this case, the Ru(IV) site must be capable of acting as an acceptor of both an electron and a proton, in addition to the detailed requirements regarding the relative orientation of reactants and the intimate association necessary to achieve the requisite electronic-vibrational coupling.

The same mechanistic complexities may also arise in electrochemical redox processes. For example, it has been suggested that for the Ru(IV)/(III) couple, $(bpy)_2(py)Ru^{IV}(O)^{2+}/(bpy)_2(py)$-$Ru^{III}(OH)^{2+}$, direct electron transfer to the electrode is slow. In fact, the direct reaction appears to be so slow that oxidation of Ru(III) and Ru(IV) occurs indirectly through the reverse of eq 7, the initial disproportionation of Ru(III) into Ru(IV) and Ru-(II)[12] (eq 8) followed by oxidation of $(bpy)_2(py)Ru(OH_2)^{2+}$ at the electrode.

$$2(bpy)_2(py)Ru(OH)^{2+} \rightarrow$$
$$(bpy)_2(py)Ru(O)^{2+} + (bpy)_2(py)Ru(OH_2)^{2+} \quad (8)$$
$$\Delta E^{\circ\prime} = 0.11 \text{ V}$$
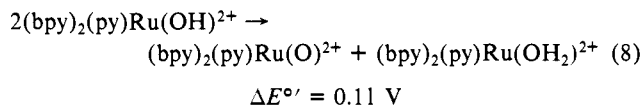
Cyclic voltammetric experiments on solutions containing $(trpy)(bpy)Ru(OH_2)^{2+}$ or $(bpy)_2(py)Ru(OH)^{2+}$[32] show that, after electrode activation, no significant decrease in ΔE_p is observed for the Ru(IV)/(III) couples. Instead, slight increases in peak currents are observed for the oxidative and reductive components for these couples as the sweep rate is lowered. The same effect is observed regardless of the details of the electrode mechanism; the fact that ΔE_p does not respond significantly to electrode activation, but the peak currents do, is consistent with the suggestion that the rate-limiting step in the overall electrochemical process is homogeneous and not heterogeneous in nature. By inference, relative to the actual electrode mechanism, direct electron transfer to and from the electrode appears to be slow, consistent with eq 8.

For the diaquo-based couples, $(by)_2(H_2O)Ru^{IV}(O)^{2+}/(bpy)_2$-$(H_2O)Ru^{III}(OH)^{2+}$ and $(bpy)_2(H_2O)Ru^{III}(OH)^{2+}/(bpy)_2$-$(H_2O)Ru^{II}(OH_2)^{2+}$, the difference in $E_{1/2}$ values between the Ru(IV)/(III) and Ru(III)/(II) couples is much larger (250 vs. 110 mV). As a consequence, a disproportionation-based pathway analogous to eq 8

$$2[(bpy)_2(H_2O)Ru(OH)]^{2+} \rightarrow$$
$$(bpy)_2(H_2O)Ru(O)^{2+} + (bpy)_2(H_2O)Ru(OH_2)^{2+}$$
$$\Delta E^{\circ\prime} = 0.25 \text{ V}$$

must be considerably slower because of the increased nonspontaneity of the initial disproportionation step. For this Ru(IV)/(III) couple, the indirect disproportionation pathway has apparently
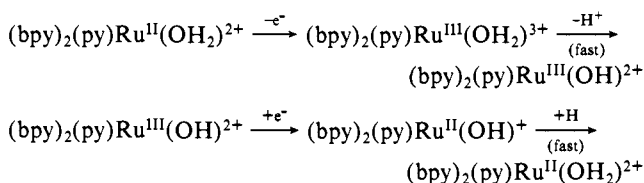
been sufficiently slowed that direct electron transfer to the electrode becomes the more facile of the two pathways. The evidence for direct electron transfer to the electrode is the dramatic decrease in ΔE_p values for the $(bpy)_2(H_2O)Ru(O)^{2+}/(bpy)_2$-$(H_2O)Ru(OH)^{2+}$ couple upon activation of the electrode (Figure 3).

Activation of the Electrode. Activation of carbon electrodes has been described based on radio frequency plasma treatment in an oxygen atmosphere[3] or by electrochemical treatment, where the effect of activation on the oxidation of ferrocyanide, hydrazine, and hydroquinone was studied systematically.[5]

Our X-ray PES data obtained for electrodes treated in a manner previously described[5,17] clearly show that the activation procedure results in the formation of oxidized carbon-based groups which are confined to within 20 nm of the electrode surface. From our results a number of conclusions can be reached. (1) Even at the plished, "unactivated" electrodes, a significant fraction of the carbon sites are oxidized. The dominant oxidized functional groups appear to be alcoholic or phenolic in nature. (2) Oxidative activation leads to noticeable increases in both alcoholic (phenolic) and ketonic (quinoidal) groups, with the ratio of oxidized to graphitic carbon atom sites increasing to nearly one-half. (3) The relatively short reductive procedure, which is necessary for the activation of the metal-based couples, leads to a significant decrease in the number of oxidized surface sites.

Origin of the Electrocatalysis. It is evident that kinetic complications can appear for electrode reactions involving redox couples where changes in proton content occur, as they do in solution. It is for just such couples that the electrode activation procedure has its largest effect and, in that context, it is important to realize that (1) even "unactivated" carbon electrodes are often necessary to observe *any* response for the redox couples. For example, it is difficult to obtain well-defined waves for Ru-(IV)/(III) couples at Pt electrodes.[10,36] (2) In the net sense, water plays a crucial role in serving both as a proton source and a proton sink. (3) Specific interaction between the components of the redox couple and the surface sites on the electrode can be important in the electrocatalysis. The evidence includes the existence of specific anion effects for the $(NH_3)_5Ru^{IV}(O)^{2+}/(NH_3)_5Ru^{III}(OH)^{2+}$ couple (Table VI) and the importance of the reductive activation cycle for the catalysis of the metal-based cationic couples. (4) The existence of significant $k_s^{H_2O}/k_s^{D_2O}$ effects suggests the possible intervention of proton-assisted electron-transfer pathways utilizing surface chemical sites on the electrodes.

As might have been expected, the specific details of the catalysis are dependent on the individual couples. For the two sets of Ru(III)/(II) based couples, $(NH_3)_5Ru^{III}(OH)^{2+}/(NH_3)_5Ru^{II}$-$(OH_2)^{2+}$ and $(bpy)_2(H_2O)Ru^{III}(OH)^{2+}/(bpy)_2(H_2O)Ru^{II}$-$(OH_2)_2)^{2+}$, the heterogeneous charge-transfer processes are nearly reversible at both polished and activated electrodes. Although there is a net proton-transfer problem associated with these couples over a broad pH range, they undergo relatively facile electron transfer irrespective of the electrode material, whether it be a platinum, gold, or carbon. Presumably, electron transfer at the electrode occurs by a simple outer-sphere mechanism, which is relatively rapid even when the extra energy associated with the additional proton in the initial redox product is taken into account, e.g.,

$$(bpy)_2(py)Ru^{II}(OH_2)^{2+} \xrightarrow{-e^-} (bpy)_2(py)Ru^{III}(OH_2)^{3+} \xrightarrow[\text{(fast)}]{-H^+}$$
$$(bpy)_2(py)Ru^{III}(OH)^{2+}$$

$$(bpy)_2(py)Ru^{III}(OH)^{2+} \xrightarrow{+e^-} (bpy)_2(py)Ru^{II}(OH)^+ \xrightarrow[\text{(fast)}]{+H}$$
$$(bpy)_2(py)Ru^{II}(OH_2)^{2+}$$

Note, however, from the data in Table V that even the Ru-(III)/(II) couples are only quasi-reversible. In fact, it is quite possible that careful measurements of heterogenous charge-transfer rate constants as a function of pH would reveal: (1) significant

increases in k_s below pH 0.85, where the dominant form of the couple is $(bpy)_2(py)Ru(OH)_2^{3+/2+}$ or above pH 10.70 where the couple is $(bpy)_2(py)Ru(OH)^{2+/+}$; and (2) pathways first order in $[H^+]$ and inverse order in $[H^+]$ as these pH regions are approached, respectively.

By contrast, a critical sensitivity to the condition of the electrode surface is exhibited by the Ru(IV)/(III) couples, $(bpy)_2(H_2O)$-$Ru(O)^{2+}/(bpy)_2(H_2O)Ru(OH)^{2+}$ and $(NH_3)_5Ru(O)^{2+}/$ $(NH_3)_5Ru(OH)^{2+}$. For these couples a single oxidative activation cycle is sufficient to cause a dramatic enhancement in the rate of electron transfer (Table IV). Compared with the Ru(III)/(II) couples, the Ru(IV)/(III) couple must have a greater inhibition to outer-sphere electron transfer, perhaps arising from enhanced vibrational trapping and a lack of a significant proton affinity by the $Ru^{IV} = O^{2+}$ group. With slow outer-sphere electron transfer, a more complex but facile proton-coupled electron transfer pathway may be utilized instead, using chemical sites at the electrode surface, e.g.,
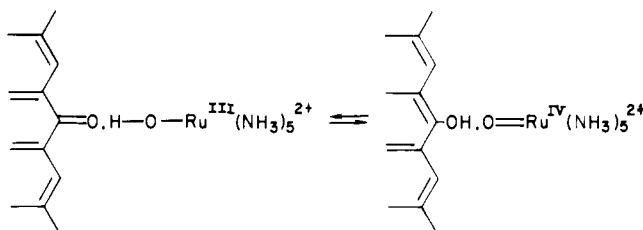
Such pathways have obvious analogues in the homogeneous reactions in eq 2 and 7.

The X-ray PES evidence for quinonal and phenolic sites at the electrode surface following the activation procedure was mentioned in the previous section. The existence of the H/D kinetic isotope effect for the pentammine couple is certainly consistent with such a conclusion. Also consistent is the existence of strong specific anion effects, since the intimate nature of the contact required for a proton-coupled electron-transfer event could be strongly influenced by anionic adsorption. In fact, the X-ray PES evidence shows that, in addition to the changes in the carbon functionalities, the reduction step removes specifically adsorbed HSO_4^- anions.

The data for the ferro/ferricyanide couple in Table VII and earlier results by Engstrom[5] show that even at pH 8.5 in 2 M KCl where ferro- and ferricyanide are fully deprotonated and two or more potassium ions are ion-paired,[37] a sensitivity to electrode activation exists (Table VII). This demonstrates that in addition to such special effects as proton-coupled electron transfer, the activation procedure must lead to significant changes at the electrode surface which can influence heterogeneous charge-transfer rates in other ways as well. Reasonable possibilities for the origin of such effects include a modification of the degree of prior association before electron transfer and/or the extent of electronic coupling between the electrode surface and the reactant.[38]

As suggested above, a complete description of the origin of the activation effect must include details beyond the simple creation of surface-active sites for proton-coupled electron transfer. The X-ray PES results suggest that such sites are present even on unactivated, polished electrodes, although probably in much smaller amounts. Significant changes in surface morphology may also occur as a consequence of the activation process. The charge density calculations of Engstrom[5] on the surface reduction wave induced by oxidative activation indicate a multilayer structure. Those calculations and the color changes observed in the activation process raise the obvious possibility that, as suggested by one of the referees, a new phase may be created where the surface has different composition from the bulk. However, the X-ray PES

---

(36) W. R. Murphy, Jr., unpublished results.

(37) W. A. Eaton, P. George, and G. I. H. Hanania, *J. Phys. Chem.*, **71**, 2016 (1967).

(38) (a) S. W. Barr, K. L. Guyer, and M. J. Weaver, *J. Electroanal. Chem.*, **111**, 41 (1980). (b) S. W. Barr, K. L. Guyer, T. T-T. Li, H. Y. Liu, and M. J. Weaver, "Proceedings of the Symposium on Chemistry and Physics of Electrocatalysis", Electrochemical Society, in press.
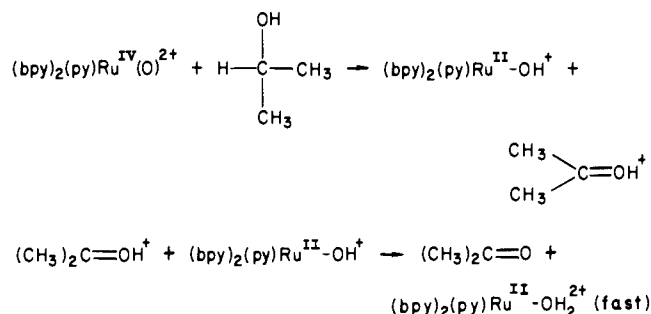
data in Table I clearly suggest that the consequences of the activation procedure are confined largely near the surface.

At the surface, the effect of oxidative activation may be to create additional "active" sites at the surface, but perhaps more importantly, to create a microenvironment near the active sites which is more conducive to the detailed mechanistic demands of the proton-coupled electron-transfer pathway. Notable in this regard is the necessity of a short-term reductive cycle following oxidative activation for the metal complex couples. Given the observation that the reductive cycle enhances the wettability of the surface, the origin of the effect may be that partial reduction creates a more hydrophilic environment at the surface,[6] which is at the same time more open and accessible to the charged metal complexes.

Other Substrates. Equally dramatic activational effects were observed for the oxidation of catechol. The importance of the specific nature of the redox couples was illustrated by the initial selective enhancement of the first of two electrochemically irreversible oxidation waves (Figure 6B). Clearly, significant catalysis of the first wave can only occur to the point that k_s approaches and becomes larger than the rate constant for diffusion to the electrode. Since the one-electron semiquinone intermediate is unstable with respect to disproportionation,[39] continued activation and therefore enhancement of k_s for the second wave ultimately leads to the observation of a two-electron process. Although the activational effects for the catechol couple are clearly consistent with the importance of proton-assisted electron transfer, the existence of adsorption effects complicates any attempt at a detailed interpretation.

The results obtained for hydrogen peroxide and isopropyl alcohol help establish the origin of the oxidation overpotential for these substrates at solid electrodes. No catalysis is observed for the oxidation of isopropyl alcohol, so it is unlikely that even a proton-assisted electron-transfer pathway is sufficiently facile to obtain significant currents. In this context it should be noted that the one-electron oxidation of isopropyl alcohol by $(bpy)_2(py)Ru^{III}OH^{2+}$ in water is apparently outer-sphere in nature[40] so that, even in the metal complex case, the proton-coupled electron transfer pathway is not sufficiently facile to make an appearance. An

additional point to consider is the fact that evidence has been obtained for the two-electron oxidation of activated organic C–H bonds,[40,41] e.g.,

$$(bpy)_2(py)Ru^{IV}(O)^{2+} + H{-}\underset{\underset{CH_3}{|}}{\overset{\overset{OH}{|}}{C}}{-}CH_3 \longrightarrow (bpy)_2(py)Ru^{II}{-}OH^+ +$$

$$\underset{CH_3}{\overset{CH_3}{>}}C{=}OH^+$$

$$(CH_3)_2C{=}OH^+ + (bpy)_2(py)Ru^{II}{-}OH^+ \longrightarrow (CH_3)_2C{=}O +$$

$$(bpy)_2(py)Ru^{II}{-}OH_2^{2+} \text{ (fast)}$$

Even though the proton-coupled electron-transfer pathways do not appear to be facile for the oxidation of isopropyl alcohol, it is conceivable that they may appear for other organic substrates.

By contrast, oxidation of H_2O_2 is *strongly* catalyzed by oxidative activation, which was noted earlier by Brezina and Hofmanova.[7] However, the most important point is the obviously large $k_s^{H_2O}/k_s^{D_2O}$ effect for the reaction. The situation at the electrode surface probably parallels that found in the oxidation of H_2O_2 by $(bpy)_2(py)RuO^{2+}$, as described in the Introduction. A key feature at the electrode surface would then become the existence of a proton-coupled electron-transfer pathway which avoids the production of the protonated perhydroxyl radical, $H_2O_2^+$.

(39) J. B. Hendrickson, D. J. Cram, and G. S. Hammond, "Organic Chemistry", McGraw-Hill, New York, 1970, pp 820–821.
(40) M. S. Thompson and T. J. Meyer, *J. Am. Chem. Soc.*, **104**, 4106 (1982).

(41) M. S. Thompson and T. J. Meyer, *J. Am. Chem. Soc.*, **104**, 5070 (1982).